Coupled Systems Mechanics, *Vol. 12, No. 1 (2023) 1-20*
https://doi.org/10.12989/csm.2023.12.1.001

Random dynamic analysis for simplified vehicle model based on explicit time-domain method

Huan Huang[a], Yuyu Li[b], Wenxiong Li* and Guihe Tang[c]

College of Water Conservancy and Civil Engineering, South China Agricultural University, Guangzhou 510642, P.R. China

(Received June 5, 2021, Revised June 15, 2022, Accepted June 21, 2022)

Abstract. On the basis of the explicit time-domain method, an investigation is performed on the influence of the rotational stiffness and rotational damping of the vehicle body and front-rear bogies on the dynamic responses of the vehicle-bridge coupled systems. The equation of motion for the vehicle subsystem is derived employing rigid dynamical theories without considering the rotational stiffness and rotational damping of the vehicle body, as well as the front-rear bogies. The explicit expressions for the dynamic responses of the vehicle and bridge subsystems to contact forces are generated utilizing the explicit time-domain method. Due to the compact wheel-rail model, which reflects the compatibility requirement of the two subsystems, the explicit expression of the evolutionary statistical moment for the contact forces may be performed with relative ease. Then, the evolutionary statistical moments for the respective responses of the two subsystems can be determined. The numerical results indicate that the simplification of vehicle model has little effect on the responses of the bridge subsystem and the vehicle body, except for the responses of the rotational degrees of freedom for the vehicle subsystem, regardless of whether deterministic or random analyses are performed.

Keywords: explicit time-domain method; random vibration analysis; simplified vehicle model; vehicle-bridge coupled system

1. Introduction

The random vibration analysis of the vehicle-bridge coupled system is one of the most prominent issues in the scientific and engineering communities (Mu *et al.* 2016, Xiao *et al.* 2019). With the rapid advancement of computer technology over the past two decades, numerical simulation technology has figured prominently in the dynamic study of the vehicle-bridge coupled system. In the meantime, whether or not the vehicle-bridge linked model used is reasonable can affect the ease of operation and rationality of the results from the calculations. The finite element modeling of the bridge subsystem has been well-developed thus far. The moving load model (Lee

*Corresponding author, Ph.D., E-mail: leewenxiong@scau.edu.cn
[a]Ph.D., E-mail: happyhuang@scau.edu.cn
[b]Ph.D., E-mail: liyuyu@scau.edu.cn
[c]Ph.D., E-mail: tguihe@scau.edu.cn

http://www.techno-press.org/?journal=csm&subpage=8 ISSN: 2234-2184 (Print), 2234-2192 (Online)

1994, Thambiratnam and Zhuge 1996), the moving mass model (Mahmoud and Zai 2002, Michaltsos *et al.* 1996), the moving oscillator model (Pesterev and Bergman 2000, Yang and Lin 2005), and the multi-body model have been applied to the physical model for the vehicle subsystem (Au *et al.* 2002, Podworna and Klasztorny 2014, Stojanovi *et al.* 2018). The rational vehicle model, which has a significant influence on the vibration of vehicle-bridge coupled systems (Deng *et al*, 2018), should be used for its subsequent convenience and effectiveness, even though the effects of various factors are expected to be accounted for in the ideal vehicle model (Zhai 2015).

As previously stated for vehicle models, the multi-body model that accurately describes the characteristics of the suspension system is a favorite among researchers (Yin *et al.* 2010, Yu *et al.* 2021, Lu *et al.* 2009, Su *et al.* 2020). However, it is still an issue for the nonlinear cases because the rotational stiffness of the vehicle body and the front-rear bogies are always coupled with their respective vertical suspension springs (see Eq. (3) in Chapter 2), which does not pose an issue for linear problems. For instance, if the vertical suspension spring shows hysteretic properties, which is a kind of coupled nonlinear problem of stiffness and damping, the rotational stiffness and the vertical stiffness will exhibit nonlinear behavior in a coupled way, resulting in a highly complex problem. Moreover, it is still a necessary work to evaluate the influences of rotational stiffness and rotational damping on the dynamic responses of the vehicle-bridge coupled system. To clarify the above issue, this paper proposes a simplified vehicle model where the rotational damping, rotational stiffness of the vehicle body, and the front-rear bogies are neglected, and further investigates the properties of the proposed simplified model.

Finally, the random vibration analysis of the entire system takes into account the random irregularity, which is the leading excitation source for the coupled vehicle-bridge system. Various techniques, such as the power spectral method (Li *et al.* 2002), the pseudo excitation method (Lu *et al.* 2009), the probability density evolution method (Yu *et al.* 2015), etc., are utilized to evaluate the random responses of the vehicle-bridge coupled systems. Notably, the physical and probabilistic mechanisms for the random vibration of the vehicle-bridge coupled system are treated in a coupled form by the aforementioned methods, resulting in a certain degree of inefficiency. In the last decade, an explicit time-domain method (ETDM) has been developed (Su *et al.* 2016, Su and Xu 2014, Su *et al.* 2020) for the uncoupled treatment of physical and probabilistic mechanisms for the random vibration analysis of linear systems and equivalent linear systems, resulting in the dimension-reduction analysis for random vibration problems. Consequently, the other purpose of this study is to evaluate the random response of the vehicle-bridge coupled system using the simplified vehicle model based on the ETDM due to its high computational efficiency. A numerical example indicates that the simplified vehicle model is feasible and effective.

2. Conventional vehicle model

The conventional multi-body model for the vehicle subsystem (Zhai 2015), which is travelling at a speed of v along the bridge subsystem, is always regarded as a multi-rigid-body system, as is shown in Fig. 1. This model consists of seven rigid bodies, including one vehicle body, one front bogie, one rear bogie, and four wheelsets. In Fig. 1, M_c and J_c denote the mass and the moment of inertia for the vehicle body, respectively; M_t and J_t are the mass and the moment of inertia for the front-rear bogies, respectively; M_w denotes the mass of each wheelset; K_{sz} and C_{sz} represent the

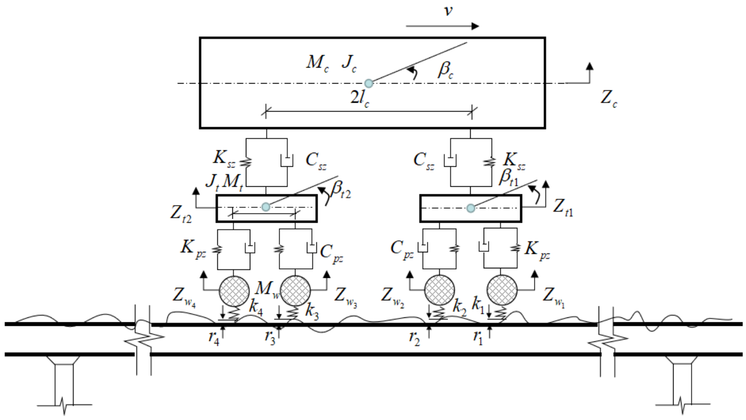

Fig. 1 Mechanical model of vehicle subsystem

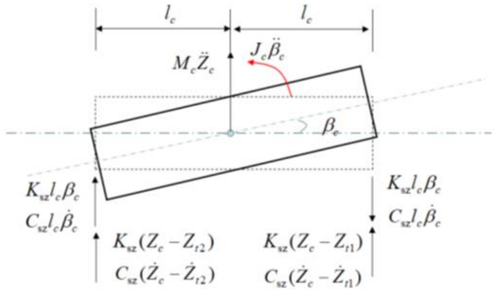

Fig. 2 Force diagram of vehicle body

vertical stiffness and damping of the secondary suspension, respectively; K_{pz} and C_{pz} represent the vertical stiffness and damping of the first suspension, respectively; Z_c denotes the vertical displacement, for which it is positive in an upward direction; β_c denotes the rotational displacement, for which it is positive in the counterclockwise direction of the vehicle body; Z_{t1} and β_{t1} represent the vertical displacement and the rotational displacement of the front bogie, respectively; Z_{t2} and β_{t2} represent the vertical displacement and the rotational displacement of the rear bogie, respectively; Z_{wi} $(i = 1, 2, 3, 4)$ denotes the displacement of each wheelset; k_i $(i = 1, 2, 3, 4)$ is the stiffness of each wheelset； r_i $(i = 1, 2, 3, 4)$ denotes the irregularity of the bridge deck. Obviously, the conventional vehicle model discussed here has 10 degrees of freedom. It should be noted that the motion of equation for the vehicle subsystem is established at the equilibrium position of the whole system. Therefore, the total weight of the vehicle subsystem is distributed evenly to the bridge subsystem through the four wheelsets.

The free-body diagram of the vehicle body is shown in Fig. 2. Based on the D'Alembert's principle, the equation of motion for the vehicle body in the vertical direction is expressed as

$$M_c\ddot{Z}_c + 2C_{sz}\dot{Z}_c - C_{sz}\dot{Z}_{t1} - C_{sz}\dot{Z}_{t2} + 2K_{sz}Z_c - K_{sz}Z_{t1} - K_{sz}Z_{t2} = 0 \tag{1}$$

Using the theorem of the moment of momentum, the equation of motion for the vehicle body in the rotational direction is given as

$$J_c\ddot{\beta}_c = -2C_{sz}l_c^2\dot{\beta}_c - 2K_{sz}l_c^2\beta_c - C_{sz}(\dot{Z}_{t_1} - \dot{Z}_{t_2})l_c - K_{sz}(Z_{t_1} - Z_{t_2})l_c \tag{2}$$

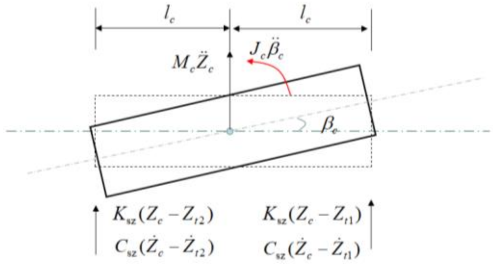

Fig. 3 Force diagram of vehicle body without considering rotational stiffness and rotational damping

Eq. (2) can be rearranged as

$$J_c\ddot{\beta}_c + 2C_{sz}l_c^2\dot{\beta}_c + 2K_{sz}l_c^2\beta_c + C_{sz}l_c\dot{Z}_{t_1} - C_{sz}l_c\dot{Z}_{t_2} + K_{sz}l_cZ_{t_1} - K_{sz}l_cZ_{t_2} = 0 \tag{3}$$

in which $2C_{sz}l_c^2$ and $2K_{sz}l_c^2$ represent the rotational damping and the rotational stiffness of the vehicle body, respectively. These two parameters are coupled with the damping and the stiffness of the vertical suspension spring, respectively.

Similar to the above deviation, the equations of motion for the front-rear bogies and the four wheelsets can be obtained easily, which can be found in the reference (Zhai 2015). As can be seen from Eq. (3), the influence of the rotational damping and the rotational stiffness of the vehicle body can be considered in this equation.

3. Simplified vehicle model

For the simplified vehicle model, the rotational dampings and the rotational stiffnesses of the vehicle body and the front-rear bogies are not taken into account. The free-body diagram of the vehicle body is shown in Fig. 3. The equation of motion for the vehicle body in the vertical direction is the same as Eq. (1), and the equation of motion for the vehicle body in the rotational direction can be expressed as

$$J_c\ddot{\beta}_c + C_{sz}l_c\dot{Z}_{t_1} - C_{sz}l_c\dot{Z}_{t_2} + K_{sz}l_cZ_{t_1} - K_{sz}l_cZ_{t_2} = 0 \tag{4}$$

The rotational damping force and the rotational restoring force have disappeared in Eq. (4) compared with Eq. (3). According to the D'Alembert's principle, it is easy to obtain the equation of motion for the front bogie in the vertical direction, namely

$$\begin{gathered} M_t\ddot{Z}_{t1} + (2C_{pz} + C_{sz})\dot{Z}_{t1} - C_{sz}\dot{Z}_c - C_{pz}\dot{Z}_{w1} - C_{pz}\dot{Z}_{w2} - K_{sz}Z_c \\ +(2K_{pz} + K_{sz})Z_{t1} - K_{pz}Z_{w1} - K_{pz}Z_{w2} = 0 \end{gathered} \tag{5}$$

Based on the theorem of the moment of momentum, the equation of motion for the front bogie in the rotational direction can be given as

$$J_t\ddot{\beta}_{t1} + C_{pz}l_t\dot{Z}_{w1} - C_{pz}l_t\dot{Z}_{w2} + K_{pz}l_tZ_{w1} - K_{pz}l_tZ_{w2} = 0 \tag{6}$$

Similarly，the equation of motion for the rear bogie in the vertical direction is expressed as

$$\begin{gathered} M_t\ddot{Z}_{t2} + (2C_{pz} + C_{sz})\dot{Z}_{t2} - C_{sz}\dot{Z}_c - C_{pz}\dot{Z}_{w3} - C_{pz}\dot{Z}_{w4} - K_{sz}Z_c \\ +(2K_{pz} + K_{sz})Z_{t2} - K_{pz}Z_{w3} - K_{pz}Z_{w4} = 0 \end{gathered} \tag{7}$$

and its equation of motion in the rotational direction can be given as

$$J_t\ddot{\beta}_{t2} + C_{pz}l_t\dot{Z}_{w3} - C_{pz}l_t\dot{Z}_{w4} + K_{pz}l_tZ_{w3} - K_{pz}l_tZ_{w4} = 0 \tag{8}$$

Lastly, all the equations of motion for the four wheelsets can be obtained based on D'Alembert's principle. The equation of motion for the first wheelset is expressed as

$$M_w\ddot{Z}_{w1} + C_{pz}\dot{Z}_{w1} + K_{pz}Z_{w1} - C_{pz}\dot{Z}_{t1} - K_{pz}Z_{t1} = F_1(t) \tag{9}$$

The equation of motion for the second wheelset is expressed as

$$M_w\ddot{Z}_{w_2} + C_{pz}\dot{Z}_{w_2} + K_{pz}Z_{w_2} - C_{pz}\dot{Z}_{t_1} - K_{pz}Z_{t_1} = F_2(t) \tag{10}$$

The equation of motion for the third wheelset is expressed as

$$M_w\ddot{Z}_{w_3} + C_{pz}\dot{Z}_{w_3} + K_{pz}Z_{w_3} - C_{pz}\dot{Z}_{t_2} - K_{pz}Z_{t_2} = F_3(t) \tag{11}$$

The equation of motion for the fourth wheelset is expressed as

$$M_w\ddot{Z}_{w_4} + C_{pz}\dot{Z}_{w_4} + K_{pz}Z_{w_4} - C_{pz}\dot{Z}_{t_2} - K_{pz}Z_{t_2} = F_4(t) \tag{12}$$

in which $F_i(t)$ ($i = 1, 2, 3, 4$) is the vehicle-bridge contact force function. The above equation can be rewritten in a matrix form as follows

$$\boldsymbol{M}_v\ddot{\boldsymbol{Y}}_v + \boldsymbol{C}_v\dot{\boldsymbol{Y}}_v + \boldsymbol{K}_v\boldsymbol{Y}_v = \boldsymbol{L}_v\boldsymbol{F}(t) \tag{13}$$

in which $\boldsymbol{Y}_v = [Z_c \;\; \beta_c \;\; Z_{t1} \;\; \beta_{t1} \;\; Z_{t2} \;\; \beta_{t2} \;\; Z_{w1} \;\; Z_{w2} \;\; Z_{w3} \;\; Z_{w4}]^T$ is the displacement vector of the vehicle subsystem; $\dot{\boldsymbol{Y}}_v$ and $\ddot{\boldsymbol{Y}}_v$ are the velocity vector and the acceleration vector of the vehicle subsystem, respectively; 'T' denotes matrix transposition; $\boldsymbol{L}_v$ is a 10×4 position matrix; $\boldsymbol{F}(t) = [F_1(t) \;\; F_2(t) \;\; F_3(t) \;\; F_4(t)]^T$; $\boldsymbol{M}_v$ is the mass matrix expressed as

$$\boldsymbol{M}_v = \begin{bmatrix} M_c & & & & & & & & & 0 \\ & J_c & & & & & & & & \\ & & M_t & & & & & & & \\ & & & J_t & & & & & & \\ & & & & M_t & & & & & \\ & & & & & J_t & & & & \\ & & & & & & M_w & & & \\ & & & & & & & M_w & & \\ & & & & & & & & M_w & \\ 0 & & & & & & & & & M_w \end{bmatrix} \tag{14}$$

$\boldsymbol{C}_v$ is the damping matrix expressed as

$$\boldsymbol{C}_v = \begin{bmatrix} 2C_{sz} & 0 & -C_{sz} & 0 & -C_{sz} & 0 & 0 & 0 & 0 & 0 \\ 0 & 0 & C_{sz}l_c & 0 & -C_{sz}l_c & 0 & 0 & 0 & 0 & 0 \\ -C_{sz} & 0 & 2C_{pz}+C_{sz} & 0 & 0 & 0 & -C_{pz} & -C_{pz} & 0 & 0 \\ 0 & 0 & 0 & 0 & 0 & 0 & C_{pz}l_t & -C_{pz}l_t & 0 & 0 \\ -C_{sz} & 0 & 0 & 0 & 2C_{pz}+C_{sz} & 0 & 0 & 0 & -C_{pz} & -C_{pz} \\ 0 & 0 & 0 & 0 & 0 & 0 & 0 & 0 & C_{pz}l_t & -C_{pz}l_t \\ 0 & 0 & -C_{pz} & 0 & 0 & 0 & C_{pz} & 0 & 0 & 0 \\ 0 & 0 & -C_{pz} & 0 & 0 & 0 & 0 & C_{pz} & 0 & 0 \\ 0 & 0 & 0 & 0 & -C_{pz} & 0 & 0 & 0 & C_{pz} & 0 \\ 0 & 0 & 0 & 0 & -C_{pz} & 0 & 0 & 0 & 0 & C_{pz} \end{bmatrix} \tag{15}$$

and $\boldsymbol{K}_v$ is the stiffness matrix expressed as

$$\boldsymbol{K}_v=\begin{bmatrix} 2K_{sz} & 0 & -K_{sz} & 0 & -K_{sz} & 0 & 0 & 0 & 0 & 0 \\ 0 & 0 & K_{sz}l_c & 0 & -K_{sz}l_c & 0 & 0 & 0 & 0 & 0 \\ -K_{sz} & 0 & 2K_{pz}+K_{sz} & 0 & 0 & 0 & -K_{pz} & -K_{pz} & 0 & 0 \\ 0 & 0 & 0 & 0 & 0 & 0 & K_{pz}l_t & -K_{pz}l_t & 0 & 0 \\ -K_{sz} & 0 & 0 & 0 & 2K_{pz}+K_{sz} & 0 & 0 & 0 & -K_{pz} & -K_{pz} \\ 0 & 0 & 0 & 0 & 0 & 0 & 0 & 0 & K_{pz}l_t & -K_{pz}l_t \\ 0 & 0 & -K_{pz} & 0 & 0 & 0 & K_{pz} & 0 & 0 & 0 \\ 0 & 0 & -K_{pz} & 0 & 0 & 0 & 0 & K_{pz} & 0 & 0 \\ 0 & 0 & 0 & 0 & -K_{pz} & 0 & 0 & 0 & K_{pz} & 0 \\ 0 & 0 & 0 & 0 & -K_{pz} & 0 & 0 & 0 & 0 & K_{pz} \end{bmatrix} \tag{16}$$

So far, one has obtained the equation of motion for the simplified vehicle subsystem, for which the rotational damping and the rotational stiffness of the vehicle body and the front-rear bogies are not taken into account.

4. Equation of motion for the bridge subsystem

Based on the conventional finite element model, it is easy to obtain the equation of motion for the bridge subsystem as

$$\boldsymbol{M}_b\ddot{\boldsymbol{Y}}_b+\boldsymbol{C}_b\dot{\boldsymbol{Y}}_b+\boldsymbol{K}_b\boldsymbol{Y}_b=\boldsymbol{L}_b(x)[-\boldsymbol{F}(t)+\boldsymbol{G}] \tag{17}$$

in which $\boldsymbol{M}_b$, $\boldsymbol{C}_b$ and $\boldsymbol{K}_b$ are the mass matrix, the damping matrix, and the stiffness matrix of the bridge subsystem, respectively; $\ddot{\boldsymbol{Y}}_b$, $\dot{\boldsymbol{Y}}_b$ and $\boldsymbol{Y}_b$ are the acceleration vector, the velocity vector, and the displacement vector, respectively; $\boldsymbol{L}_b(x)$ is the position matrix which is related to the position of the wheel sets. $\boldsymbol{G}=[\mathrm{G}\ \ \mathrm{G}\ \ \mathrm{G}\ \ \mathrm{G}]^T$ is the gravity vector in which G=(M_c+2M_t+4M_w)g/4 with g being the gravity acceleration.

The vehicle subsystem and the bridge subsystem are coupled via the contact force $\boldsymbol{F}(t)$, which is determined by the following compatibility equation

$$y_{\mathrm{v},\,i}(t)-y_{\mathrm{b},\,i}(x,t)-r_i(x)=-\frac{F_i(t)}{k_i}\ \ (i=1,2,3,4) \tag{18}$$

in which $y_{\mathrm{v},\,i}(t)$ is the vertical displacement of the i-th wheelset; $y_{\mathrm{b},\,i}(x,t)$ is the vertical displacement of the bridge deck corresponding to the i-th wheelset; $r_i(x)$ is the irregularity of the bridge deck corresponding to the i-th wheelset.

5. Random dynamic analysis based on the ETDM

5.1 Explicit expression of responses for the vehicle subsystem

In this section, the Newmark-β method is used to solve the equation of motion for the simplified vehicle subsystem shown in Eq. (13). For the Newmark-β method, the following assumptions are used as follows (Bathe 1996, Li and Ma 2019)

$$\dot{\boldsymbol{Y}}_{\mathrm{v},\,j}=\dot{\boldsymbol{Y}}_{\mathrm{v},\,j-1}+[(1-\gamma)\ddot{\boldsymbol{Y}}_{\mathrm{v},\,j-1}+\gamma\ddot{\boldsymbol{Y}}_{\mathrm{v},\,j}]\Delta t\ \ (j=1,2,\cdots,n) \tag{19}$$

$$\boldsymbol{Y}_{\mathrm{v},\,j}=\boldsymbol{Y}_{\mathrm{v},\,j-1}+\dot{\boldsymbol{Y}}_{\mathrm{v},\,j-1}\Delta t+\frac{1}{2}[(1-2\beta)\ddot{\boldsymbol{Y}}_{\mathrm{v},\,j-1}+2\beta\ddot{\boldsymbol{Y}}_{\mathrm{v},\,j}]\Delta t^2\ \ (j=1,2,\cdots,n) \tag{20}$$

where $n=T/\Delta t$ with T and Δt being the total time and the time step, respectively; the subscripts "$j-1$" and "j" denote $t_{j-1}=(j-1)\Delta t$ and $t_j=j\Delta t$, respectively; $\boldsymbol{Y}_{\mathrm{v},\,j-1}=\boldsymbol{Y}_v(t_{j-1})$ and $\boldsymbol{Y}_{\mathrm{v},\,j}=\boldsymbol{Y}_v(t_j)$; γ and β are two parameters used to control the Newmark-β integration stability. In this study, $\gamma=0.5$ and $\beta=0.25$ are used and the Newmark-β method will be unconditionally stable. Based on Eqs. (19) and (20), one can obtain the acceleration and the velocity at time instant t_j and they can be expressed as

$$\ddot{\boldsymbol{Y}}_{\mathrm{v},\,j}=a_0(\boldsymbol{Y}_{\mathrm{v},\,j}-\boldsymbol{Y}_{\mathrm{v},\,j-1})-a_1\dot{\boldsymbol{Y}}_{\mathrm{v},\,j-1}-a_2\ddot{\boldsymbol{Y}}_{\mathrm{v},\,j-1}\ \ (j=1,2,\cdots,n) \tag{21}$$

$$\dot{\boldsymbol{Y}}_{\mathrm{v},\,j}=a_3(\boldsymbol{Y}_{\mathrm{v},\,j}-\boldsymbol{Y}_{\mathrm{v},\,j-1})-a_4\dot{\boldsymbol{Y}}_{\mathrm{v},\,j-1}-a_5\ddot{\boldsymbol{Y}}_{\mathrm{v},\,j-1}\ \ (j=1,2,\cdots,n) \tag{22}$$

where

$$\begin{cases} a_0=\frac{1}{\beta\Delta t^2},a_1=\frac{1}{\beta\Delta t},a_2=\frac{1}{2\beta}-1 \\ a_3=\frac{\gamma}{\beta\Delta t},a_4=\frac{\gamma}{\beta}-1,a_5=\frac{\Delta t}{2}(\frac{\gamma}{\beta}-2) \end{cases} \tag{23}$$

The equation of motion for the equivalent linear vehicle subsystem at time instant t_j can be written as

$$\boldsymbol{M}_v\ddot{\boldsymbol{Y}}_{\mathrm{v},\,j}+\boldsymbol{C}_v\dot{\boldsymbol{Y}}_{\mathrm{v},\,j}+\boldsymbol{K}_v\boldsymbol{Y}_{\mathrm{v},\,j}=\boldsymbol{L}_v\boldsymbol{F}_j \tag{24}$$

By substituting Eqs. (21) and (22) into Eq. (24), it yields

$$\boldsymbol{Y}_{\mathrm{v},\,j}=\widehat{\boldsymbol{K}}^{-1}\widehat{\boldsymbol{F}}_j \tag{25}$$

where

$$\widehat{\boldsymbol{K}}=\boldsymbol{K}_v+a_0\boldsymbol{M}_v+a_3\boldsymbol{C}_v \tag{26}$$

$$\widehat{\boldsymbol{F}}_j=\boldsymbol{L}_v\boldsymbol{F}_j+\boldsymbol{M}_v(a_0\boldsymbol{Y}_{\mathrm{v},\,j-1}+a_1\dot{\boldsymbol{Y}}_{\mathrm{v},\,j-1}+a_2\ddot{\boldsymbol{Y}}_{\mathrm{v},\,j-1})+\boldsymbol{C}_v(a_3\boldsymbol{Y}_{\mathrm{v},\,j-1}+a_4\dot{\boldsymbol{Y}}_{\mathrm{v},\,j-1}+a_5\ddot{\boldsymbol{Y}}_{\mathrm{v},\,j-1}) \tag{27}$$

In addition, based on Eq. (24), the acceleration vector at time instant t_j can also be expressed as

$$\ddot{\boldsymbol{Y}}_{\mathrm{v},\,j}=\boldsymbol{M}_v^{-1}[\boldsymbol{L}_v\boldsymbol{F}_j-\boldsymbol{C}_v\dot{\boldsymbol{Y}}_{\mathrm{v},\,j}-\boldsymbol{K}_v\boldsymbol{Y}_{\mathrm{v},\,j}] \tag{28}$$

Analogously, one has

$$\ddot{\boldsymbol{Y}}_{\mathrm{v},\,j-1}=\boldsymbol{M}_v^{-1}[\boldsymbol{L}_v\boldsymbol{F}_{j-1}-\boldsymbol{C}_v\dot{\boldsymbol{Y}}_{\mathrm{v},\,j-1}-\boldsymbol{K}_v\boldsymbol{Y}_{\mathrm{v},\,j-1}] \tag{29}$$

By substituting Eq. (29) into Eq. (27), it yields

$$\boldsymbol{Y}_{\mathrm{v},\,j}=\boldsymbol{H}_{11}\boldsymbol{Y}_{\mathrm{v},\,j-1}+\boldsymbol{H}_{12}\dot{\boldsymbol{Y}}_{\mathrm{v},\,j-1}+\boldsymbol{R}_1\boldsymbol{L}_v\boldsymbol{F}_{j-1}+\boldsymbol{R}_2\boldsymbol{L}_v\boldsymbol{F}_j \tag{30}$$

where

$$\begin{cases} \boldsymbol{H}_{11}=\hat{\boldsymbol{K}}^{-1}(\boldsymbol{S}_1-\boldsymbol{S}_3\boldsymbol{M}_{\mathrm{v}}^{-1}\boldsymbol{K}_{\mathrm{v}}),\ \boldsymbol{H}_{12}=\hat{\boldsymbol{K}}^{-1}[\boldsymbol{S}_2-\boldsymbol{S}_3\boldsymbol{M}_{\mathrm{v}}^{-1}\boldsymbol{C}_{\mathrm{v}}] \\ \boldsymbol{R}_1=\hat{\boldsymbol{K}}^{-1}\boldsymbol{S}_3\boldsymbol{M}_{\mathrm{v}}^{-1},\ \boldsymbol{R}_2=\hat{\boldsymbol{K}}^{-1} \\ \boldsymbol{S}_1=a_0\boldsymbol{M}_{\mathrm{v}}+a_3\boldsymbol{C}_{\mathrm{v}},\ \boldsymbol{S}_2=a_1\boldsymbol{M}_{\mathrm{v}}+a_4\boldsymbol{C}_{\mathrm{v}},\ \boldsymbol{S}_3=a_2\boldsymbol{M}_{\mathrm{v}}+a_5\boldsymbol{C}_{\mathrm{v}} \end{cases} \tag{31}$$

By substituting Eq. (30) into (22) and considering Eq. (29), it yields

$$\dot{\boldsymbol{Y}}_{\mathrm{v},\,j}=\boldsymbol{H}_{21}\boldsymbol{Y}_{\mathrm{v},\,j-1}+\boldsymbol{H}_{22}\dot{\boldsymbol{Y}}_{\mathrm{v},\,j-1}+\boldsymbol{R}_3\boldsymbol{L}_v\boldsymbol{F}_{j-1}+\boldsymbol{R}_4\boldsymbol{L}_v\boldsymbol{F}_j \tag{32}$$

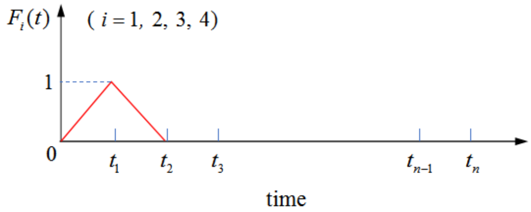

Fig. 4 A unit impulse of the wheel-bridge contact force

where

$$\begin{cases} \boldsymbol{H}_{21} = a_3(\boldsymbol{H}_{11} - \mathbf{I}) + a_5 \boldsymbol{M}_{\mathrm{v}}^{-1}\boldsymbol{K}_{\mathrm{v}},\ \boldsymbol{H}_{22} = a_3\boldsymbol{H}_{12} - a_4\mathbf{I} + a_5\boldsymbol{M}_{\mathrm{v}}^{-1}\boldsymbol{C}_{\mathrm{v}} \\ \boldsymbol{R}_3 = a_3\boldsymbol{R}_1 - a_5\boldsymbol{M}_{\mathrm{v}}^{-1},\ \boldsymbol{R}_4 = a_3\boldsymbol{R}_2 \end{cases} \tag{33}$$

in which I is the identity matrix.

Based on Eqs. (30) and (32), one can derive the following recursion formula

$$\boldsymbol{V}_v(t_j) = \boldsymbol{T}_v\boldsymbol{V}_{\mathrm{v},\, j-1} + \boldsymbol{Q}_{\mathrm{v}1}F_{j-1} + \boldsymbol{Q}_{\mathrm{v}2}F_j \quad (j = 1, 2, \cdots, n) \tag{34}$$

where

$$\boldsymbol{V}_v = \begin{Bmatrix} \boldsymbol{Y}_v \\ \dot{\boldsymbol{Y}}_v \end{Bmatrix} \tag{35}$$

and $\boldsymbol{T}_v$, $\boldsymbol{Q}_{\mathrm{v}1}$ and $\boldsymbol{Q}_{\mathrm{v}2}$ are given as follows

$$\boldsymbol{T}_v = \begin{bmatrix} \boldsymbol{H}_{11} & \boldsymbol{H}_{12} \\ \boldsymbol{H}_{21} & \boldsymbol{H}_{22} \end{bmatrix}, \boldsymbol{Q}_{v1} = \begin{bmatrix} \boldsymbol{R}_1 \\ \boldsymbol{R}_3 \end{bmatrix}\boldsymbol{L}_v, \boldsymbol{Q}_{v2} = \begin{bmatrix} \boldsymbol{R}_2 \\ \boldsymbol{R}_4 \end{bmatrix}\boldsymbol{L}_v \tag{36}$$

Without loss of generality, $V_v(t_0) = \mathbf{0}$ and $\ddot{\boldsymbol{Y}}00_v$ are assumed. Then, based on Eq. (34), the explicit expression for the state vector $\boldsymbol{V}_v$ at t_j can be written as (Su *et al.* 2016, 2020, Su and Xu 2014)

$$\boldsymbol{V}_v(t_j) = \boldsymbol{A}_{v(j,1)}\boldsymbol{F}_1 + \boldsymbol{A}_{v(j,2)}\boldsymbol{F}_2 + \cdots + \boldsymbol{A}_{v(j,j)}\boldsymbol{F}_j \quad (j = 1, 2, \cdots, n) \tag{37}$$

where $\boldsymbol{A}_{\mathrm{v}(j,p)}$ $(p = 1,2,\cdots,j)$ are the coefficient matrices and they are expressed in closed forms as (Su *et al.* 2014, 2016, 2020)

$$\boldsymbol{A}_{v(j,j)} = \boldsymbol{Q}_{v2},\ \mathbf{A}_{v(j,j-1)} = \boldsymbol{T}_v\boldsymbol{Q}_{v2} + \boldsymbol{Q}_{v1},\ \mathbf{A}_{v(j,j-k)} = \boldsymbol{T}_v\boldsymbol{A}_{v(j,j-k+1)}\ (k = 2, \cdots, j) \tag{38}$$

The coefficient matrices $\boldsymbol{A}_{v(j,p)}$ $(p = 1, 2, \cdots, j)$ can be obtained in another way (Huang *et al.* 2022, Su and Xu 2014, Su *et al.* 2020). These coefficient matrices are equivalent to the responses of the vehicle subsystem exerted by a unit impulse of the wheel-bridge contact force $F_i(t)$ $(i = 1, 2, 3, 4)$ applied at $t = t_1$ shown in Fig. 4. In this study, the coefficient matrices $\boldsymbol{A}_{\mathrm{v}(j,p)}$ $(p = 1,2,\cdots,j)$ are constructed via the way of a unit impulse applied to each wheelset, which will be given in detail in Section 5.4.

5.2 Explicit expression of responses for the bridge subsystem

In light of the derivation process of the explicit expression for the state vector $\boldsymbol{V}_v(t_j)$ expressed by Eq. (37), one can obtain the explicit expression of the bridge subsystem at the concerned time instant t_j in the same way as follows

$$\boldsymbol{V}_b(t_j) = \boldsymbol{A}_{b(j,1)}(\boldsymbol{F}_1 - \boldsymbol{G}) + \boldsymbol{A}_{b(j,2)}(\boldsymbol{F}_2 - \boldsymbol{G}) + \cdots + \boldsymbol{A}_{b(j,j)}(\boldsymbol{F}_j - \boldsymbol{G}) \tag{39}$$

where $\boldsymbol{V}_b(t_j)$ is the state vector of the bridge subsystem expressed by $\boldsymbol{V}_b(t_j) = [\boldsymbol{Y}_b^T(t_j)\ \dot{\mathbf{Y}}_b^T(t_j)]^T$; $\boldsymbol{A}_{b(j,p)}$ $(p = 1, 2, \cdots, j)$ represents the state matrices consisting of four state vectors at a time instant $t = t_p(p = 1, 2, \cdots, j)$ exerted by an impulse of the wheel-bridge contact force $F_i(t_p)(i = 1, 2, 3, 4)$. In other words, if there are j time instants, there will be $4j = 4 \times j$ wheel-bridge contact points. Therefore, to obtain $\boldsymbol{A}_{b(j,1)}$, $\boldsymbol{A}_{b(j,2)}$, $\cdots$, $\boldsymbol{A}_{b(j,j)}$, it needs nearly $4j$-times determinate dynamic history analyses for the bridge subsystem.

5.3 Explicit expression of contact forces

Eq. (37) and Eq. (39) can be expressed in a compact form as

$$\boldsymbol{V}_v(t_j) = \boldsymbol{A}_{vj}\boldsymbol{F}_{1-j}\ (j = 1, 2, \cdots, n) \tag{40}$$

$$\boldsymbol{V}_b(t_j) = \boldsymbol{A}_{bj}(\boldsymbol{F}_{1-j} - \boldsymbol{G}_{1-j})\ (j = 1, 2, \cdots, n) \tag{41}$$

where $\boldsymbol{F}_{1-j} = [\boldsymbol{F}^T(t_1)\ \mathbf{F}^T(t_2)\ \cdots\ \mathbf{F}^T(t_j)]^T$; $\boldsymbol{G}_{1-j} = [\boldsymbol{G}_1^T\ \mathbf{G}_2^T\ \cdots\ \mathbf{G}_j^T]^T$; $\boldsymbol{A}_{vj} = [\boldsymbol{A}_{v(j,1)}\ \boldsymbol{A}_{v(j,2)}\ \cdots\ \boldsymbol{A}_{v(j,j)}]$ and $\boldsymbol{A}_{bj} = [\boldsymbol{A}_{b(j,1)}\ \boldsymbol{A}_{b(j,2)}\ \cdots\ \boldsymbol{A}_{b(j,j)}]$.

Considering the compatibility equation expressed by Eq. (18) at all of the time instants, let the stiffness of each wheelset $k_i = k$ $(i = 1, 2, 3, 4)$, one can obtain the following equation

$$\boldsymbol{y}_{\mathrm{v},\,1\text{-}n} - \boldsymbol{y}_{\mathrm{b},\,1\text{-}n} - \boldsymbol{r}_{1\text{-}n} = -\frac{\boldsymbol{F}_{1\text{-}n}}{k} \tag{42}$$

where $\boldsymbol{y}_{\mathrm{v},\,1\text{-}n} = [\boldsymbol{y}_{\mathrm{v},\,1}\ \mathbf{y}_{\mathrm{v},\,2}\ \cdots\ \mathbf{y}_{\mathrm{v},\,n}]^T$ in which $\boldsymbol{y}_{\mathrm{v},\,j} = [y_{v,1}(t_j)\ \ y_{v,2}(t_j)\ \ y_{v,3}(t_j)\ \ y_{v,4}(t_j)]$ $(j = 1, 2, \cdots, n)$ is the vertical displacements of the four wheelsets at the same time instant; $\boldsymbol{y}_{\mathrm{b},\,1\text{-}n} = [\boldsymbol{y}_{\mathrm{b},\,1}\ \mathbf{y}_{\mathrm{b},\,2}\ \cdots\ \mathbf{y}_{\mathrm{b},\,n}]^T$ in which $\boldsymbol{y}_{\mathrm{b},\,j} = [y_{b,1}(t_j)\ \ y_{b,2}(t_j)\ \ y_{b,3}(t_j)\ \ y_{b,4}(t_j)](j = 1, 2, \cdots, n)$ is the vertical displacements of the bridge deck corresponding to the wheel-bridge contact points; $\boldsymbol{r}_{1\text{-}n} = [\boldsymbol{r}_1\ \mathbf{r}_2\ \cdots\ \mathbf{r}_n]^T$ in which $\boldsymbol{r}_j = [r_1(x_j)\ r_2(x_j)\ r_3(x_j)\ r_4(x_j)](j = 1, 2, \cdots, n)$ represents the irregularities of the bridge deck corresponding to the wheel-bridge contact points.

Based on Eq. (40), one can obtain the expression of $\boldsymbol{y}_{\mathrm{v},\,1\text{-}n}$ as

$$\boldsymbol{y}_{\mathrm{v},\,1\text{-}n} = \boldsymbol{A}_{v,\ \mathrm{w}}\boldsymbol{F}_{1-n} \tag{43}$$

where $\boldsymbol{A}_{v,\ \mathrm{w}}$ is extracted from $\boldsymbol{A}_{vj}(j = 1, 2, \cdots, n)$. Similarly, $\boldsymbol{y}_{\mathrm{b},\,1\text{-}n}$ can be given as

$$\boldsymbol{y}_{\mathrm{b},\,1\text{-}n} = \boldsymbol{A}_{b,\ \mathrm{w}}\boldsymbol{F}_{1-n} \tag{44}$$

where $\boldsymbol{A}_{b,\ \mathrm{w}}$ is extracted from $\boldsymbol{A}_{bj}(j = 1, 2, \cdots, n)$. Substituting Eqs. (43) and (44) into Eq. (42), one can obtain

$$\boldsymbol{F}_{1\text{-}n} = \boldsymbol{A}\boldsymbol{r}_{1\text{-}n} + \boldsymbol{B} \tag{45}$$

in which

$$\boldsymbol{A}=\left(\boldsymbol{A}_{v,\ \mathrm{w}}-\boldsymbol{A}_{b,\ \mathrm{w}}+\frac{\boldsymbol{I}}{k}\right)^{-1}$$
$$\boldsymbol{B}=-\boldsymbol{A}\boldsymbol{A}_{b,\ \mathrm{w}}\boldsymbol{G}_{1-n} \tag{46}$$

Thus far, the physical evolutionary for the dynamic responses of the vehicle-bridge coupled system has been accomplished, as is shown by Eq. (40), Eq. (41) and Eq. (45). According to the operation rules of the moments, the mean vector and the correlation matrix of the contact forces $\boldsymbol{F}_{1\text{-}n}$ can be obtained based on Eq. (45) as follows

$$E(\boldsymbol{F}_{1\text{-}n})=\boldsymbol{A}E(\boldsymbol{r}_{1\text{-}n})+\boldsymbol{B} \tag{47}$$

$$\mathrm{cov}(\mathbf{F}_{1\text{-}n},\mathbf{F}_{1\text{-}n})=\boldsymbol{A}\mathrm{cov}(\mathbf{r}_{1\text{-}n},\mathbf{r}_{1\text{-}n})\boldsymbol{A}^{T} \tag{48}$$

where $E(\boldsymbol{r}_{1\text{-}n})$ and $\mathrm{cov}(\mathbf{r}_{1\text{-}n},\mathbf{r}_{1\text{-}n})$ represent the mean vector and the covariance matrix of the irregularity vector $\boldsymbol{r}_{1\text{-}n}$ of the bridge deck which are expressed as

$$E(\boldsymbol{r}_{1\text{-}n})=[\boldsymbol{\mu}(\boldsymbol{r}_1)\ \ \boldsymbol{\mu}(\mathbf{r}_2)\ \ \cdots\ \ \boldsymbol{\mu}(\mathbf{r}_n)]^{T} \tag{49}$$

$$cov(\boldsymbol{r}_{1\text{-}n},\boldsymbol{r}_{1\text{-}n})=\begin{bmatrix}\boldsymbol{R}(\boldsymbol{r}_1,\boldsymbol{r}_1)-\boldsymbol{\mu}^T(\boldsymbol{r}_1)\boldsymbol{\mu}(\boldsymbol{r}_1) & \boldsymbol{R}(\boldsymbol{r}_1,\boldsymbol{r}_2)-\boldsymbol{\mu}^T(\boldsymbol{r}_1)\boldsymbol{\mu}(\boldsymbol{r}_2) & \cdots & \boldsymbol{R}(\boldsymbol{r}_1,\boldsymbol{r}_n)-\boldsymbol{\mu}^T(\boldsymbol{r}_1)\boldsymbol{\mu}(\boldsymbol{r}_n)\\ \boldsymbol{R}(\boldsymbol{r}_2,\boldsymbol{r}_1)-\boldsymbol{\mu}^T(\boldsymbol{r}_2)\boldsymbol{\mu}(\boldsymbol{r}_1) & \boldsymbol{R}(\boldsymbol{r}_2,\boldsymbol{r}_2)-\boldsymbol{\mu}^T(\boldsymbol{r}_2)\boldsymbol{\mu}(\boldsymbol{r}_2) & \cdots & \boldsymbol{R}(\boldsymbol{r}_2,\boldsymbol{r}_n)-\boldsymbol{\mu}^T(\boldsymbol{r}_2)\boldsymbol{\mu}(\boldsymbol{r}_n)\\ \vdots & \vdots & \ddots & \vdots\\ \boldsymbol{R}(\boldsymbol{r}_n,\boldsymbol{r}_1)-\boldsymbol{\mu}^T(\boldsymbol{r}_n)\boldsymbol{\mu}(\boldsymbol{r}_1) & \boldsymbol{R}(\boldsymbol{r}_n,\boldsymbol{r}_2)-\boldsymbol{\mu}^T(\boldsymbol{r}_n)\boldsymbol{\mu}(\boldsymbol{r}_2) & \cdots & \boldsymbol{R}(\boldsymbol{r}_n,\boldsymbol{r}_n)-\boldsymbol{\mu}^T(\boldsymbol{r}_n)\boldsymbol{\mu}(\boldsymbol{r}_n)\end{bmatrix} \tag{50}$$

where $\boldsymbol{\mu}(\boldsymbol{r}_j)=\{E[r_1(x_j)]\ \ E[r_2(x_j)]\ \ E[r_3(x_j)]\ \ E[r_4(x_j)]\}$ $(j=1,2,\cdots,n)$with $E[r_i(x_j)]$ $(i=1,2,3,4)$being the mean function of the bridge undulation; $\boldsymbol{R}(\boldsymbol{r}_k,\boldsymbol{r}_j)$ $(k=1,2,\cdots,n;\ j=1,2,\cdots,n)$ can be written as

$$\boldsymbol{R}(\boldsymbol{r}_k,\boldsymbol{r}_j)=\begin{bmatrix}E[r_1(x_k)r_1(x_j)] & E[r_1(x_k)r_2(x_j)] & E[r_1(x_k)r_3(x_j)] & E[r_1(x_k)r_4(x_j)]\\ E[r_2(x_k)r_1(x_j)] & E[r_2(x_k)r_2(x_j)] & E[r_2(x_k)r_3(x_j)] & E[r_2(x_k)r_4(x_j)]\\ E[r_3(x_k)r_1(x_j)] & E[r_3(x_k)r_2(x_j)] & E[r_3(x_k)r_3(x_j)] & E[r_3(x_k)r_4(x_j)]\\ E[r_4(x_k)r_1(x_j)] & E[r_4(x_k)r_2(x_j)] & E[r_4(x_k)r_3(x_j)] & E[r_4(x_k)r_4(x_j)]\end{bmatrix} \tag{51}$$

in which $E[r_i(x_k)r_l(x_j)](i=1,2,3,4;\ l=1,2,3,4)$ is the correlation function of the bridge undulation.

For most situations, not all dynamic responses need to be taken into account. For instance, one may be concerned about some responses, e.g., $\tilde{y}_v$ and $\tilde{y}_b$, which are any response of the vehicle subsystem and any response of the bridge subsystem, respectively. $\tilde{y}_v$ and $\tilde{y}_b$ can be expressed as

$$\tilde{y}_v(t_j)=\widetilde{\boldsymbol{A}}_{vj}\boldsymbol{F}_{1-j}\ (j=1,2,\cdots,n) \tag{52}$$

$$\tilde{y}_b(t_j)=\widetilde{\boldsymbol{A}}_{bj}(\boldsymbol{F}_{1-j}-\boldsymbol{G}_{1-j})\ (j=1,2,\cdots,n) \tag{53}$$

where $\widetilde{\boldsymbol{A}}_{vj}$ and $\widetilde{\boldsymbol{A}}_{bj}$ are both row vectors which are extracted from $\boldsymbol{A}_{vj}$ in Eq.(43) and $\boldsymbol{A}_{bj}$ in Eq.(44) , respectively. Then, based on the operation rules of the 1-st and 2-second order moments, one can obtain the mean and the covariance of $\tilde{y}_v$ and $\tilde{y}_b$ using Eqs. (52) and (53) as

$$\begin{cases}\mu_{\tilde{y}_v}(t_j) = \widetilde{\boldsymbol{A}}_{vj}E(\boldsymbol{F}_{1-j}) \\ \sigma^2_{\tilde{y}_v} = \widetilde{\boldsymbol{A}}_{vj}\mathrm{cov}(\mathbf{F}_{1-j}, \mathbf{F}_{1-j})\widetilde{\boldsymbol{A}}^T_{vj}\end{cases} (j = 1, 2, \cdots, n) \tag{54}$$

$$\begin{cases}\mu_{\tilde{y}_b}(t_j) = \widetilde{\boldsymbol{A}}_{bj}[E(\boldsymbol{F}_{1-j}) - \boldsymbol{G}_{1-j}] \\ \sigma^2_{\tilde{y}_b} = \widetilde{\boldsymbol{A}}_{bj}\mathrm{cov}(\mathbf{F}_{1-j}, \mathbf{F}_{1-j})\widetilde{\boldsymbol{A}}^T_{bj}\end{cases} (j = 1, 2, \cdots, n) \tag{55}$$

It is noted that Eqs. (54) and (55) reflect the probabilistic evolutionary mechanisms of dynamic responses. Because of the uncoupled treatment of the physical evolutionary and the probabilistic evolutionary mechanisms for the dynamic responses of the system, the dimension-reduction analysis for the responses concerned can be carried out based on Eqs. (54) and (55). This kind of uncoupled treatment for the two mechanisms greatly improves the calculational efficiency (Su *et al.* 2016, 2020, Su and Xu 2014).

5.4 Solution procedure for vehicle-bridge coupled system

To illustrate the solution procedure discussed above, the detailed solving steps are given as follows:

(1) Assign a unit impulse to one wheelset with the remaining wheelsets being applied by zero loads, and calculate the time histories of displacements, velocities, and accelerations of the vehicle subsystem.

(2) Repeat step (1) from the first wheelset to the fourth wheelset, and construct the coefficient matrices $\boldsymbol{A}_{vj}$ $(j = 1,2,\cdots,n)$ in Eq. (37) for the vehicle subsystem.

(3) Extract $\boldsymbol{A}_{v,\ w}$ in Eq. (43) from $\boldsymbol{A}_{vj}(j = 1, 2, \cdots, n)$.

(4) Assign a unit impulse to the contact point attached to the bridge deck, which is corresponding to the first wheelset, and calculate the time histories of displacements, velocities, and accelerations for all the degrees of freedom of the bridge. Then, one can construct the first column vector of coefficient matrices $\boldsymbol{A}_{bj}$ $(j = 1,2,\cdots,n)$ in Eq. (39) for the bridge subsystem.

(5) Repeat step (4) according to the order of wheelsets, and construct the remaining column vectors of coefficient matrices $\boldsymbol{A}_{bj}$ $(j = 1,2,\cdots,n)$ in Eq. (39) for the bridge subsystem.

(6) Extract $\boldsymbol{A}_{b,\ w}$ in Eq. (44) from $\boldsymbol{A}_{bj}(j = 1, 2, \cdots, n)$. It is noted that the vertical displacements of the contact points do not always fall onto the nodes. In such a case, the vertical displacements of the contact points can be constructed through the interpolation function between the two adjacent nodes, which can be found in the reference (Huang *et al.* 2022).

(7) Calculate matrices $\boldsymbol{A}$ and $\boldsymbol{B}$ based on (46).

(8) The mean vector and the correlation matrix of the contact forces $\boldsymbol{F}_{1\text{-}n}$ can be obtained based on Eqs. (47) and (48), respectively.

(9) The concerned responses can be calculated based on Eqs. (54) and (55).

A simple flow chart shown in Fig. 5 can be used to represent the above calculation steps.

6. Numerical examples

In the following numerical example, a simply supported beam is used in the vehicle-bridge coupled system as shown in Fig. 6. Most parameters used in this example are from the work of Su

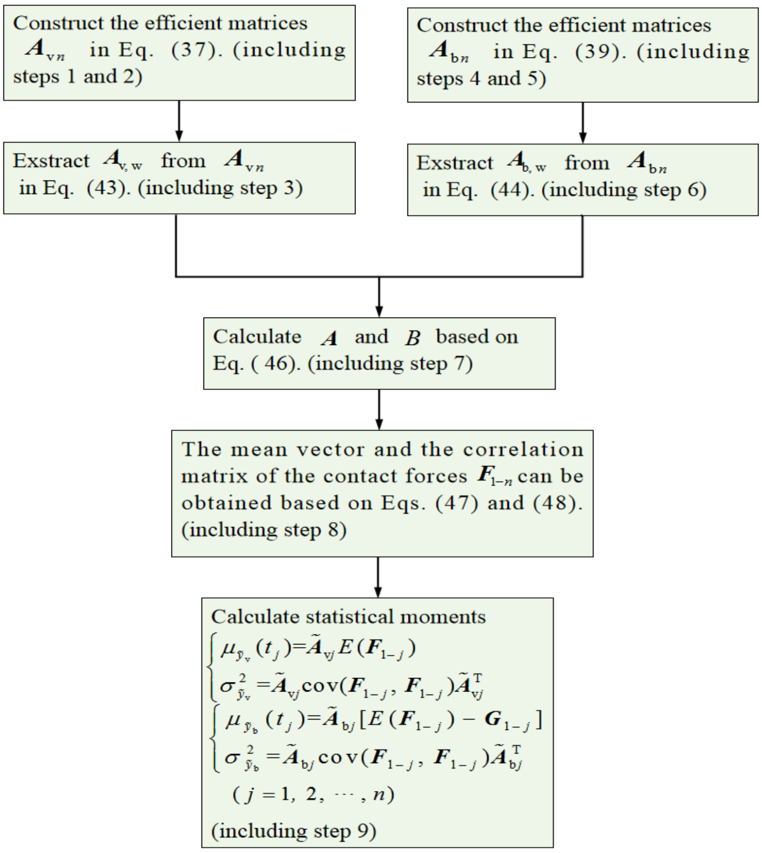

Fig. 5 The flowchart of the solution procedure

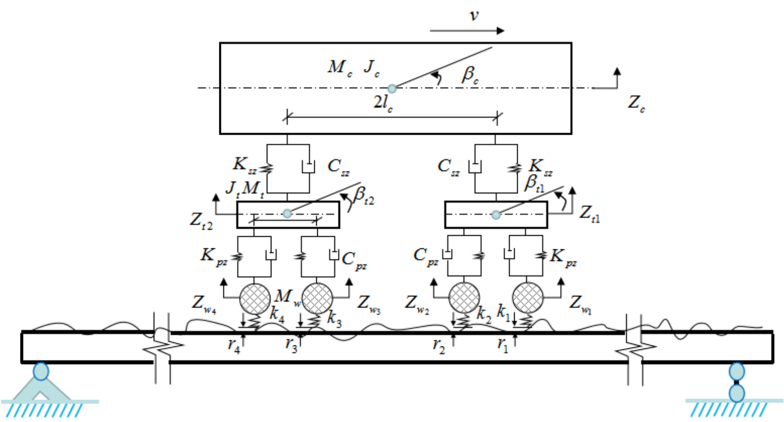

Fig. 6 Mechanical model of a coupled vehicle-bridge system

et al. (2020). Data for the vehicle model is given in Table 1. The length of the bridge in the model is set to be $L = 100$ m. Its bending stiffness is $EI = 2658069$ kN/m and the linear density is $\rho A = 6067$ kg/m. The damping of the bridge is overlooked. The bridge subsystem is modeled by

Table 1 Structural parameters of the vehicle model

parameter symbol	value	unit	parameter symbol	value	unit
M_c	34231	kg	J_t	3930	kg · m^2
J_c	20800	kg · m^2	l_t	1.25	m
l_c	11.95	m	K_{pz}	808740	N/m
K_{sz}	180554	N/m	C_{pz}	7500	N · s
C_{sz}	16250	N · s/m	M_w	1583	kg
M_t	2760	kg	$k_1 = k_2 = k_3 = k_4$	2005.540	N/m

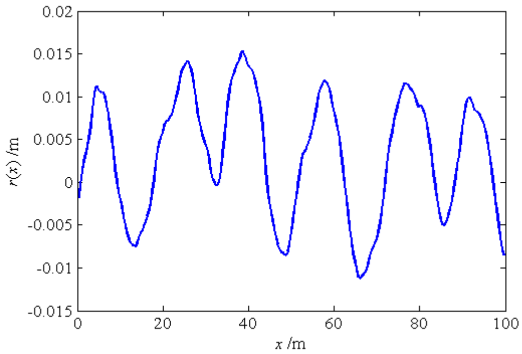

Fig. 7 An irregularity sample

50 plane beam elements.

The bridge undulation $r(x)$ is supposed to be a homogeneous Gaussian random field with a zero mean value and its power spectral density is expressed by

$$S(\omega) = \frac{1}{\pi} \frac{4\gamma\beta\chi\omega_0^2}{(\omega_0^2 - \omega^2)^2 + 4\beta^2\omega^2} \tag{56}$$

where $\omega_0^2 = \beta^2 + \chi^2$, $\beta = 0.1$, $\chi = 0.3$ and $\gamma = 1\ \mathrm{cm}^2 \cdot \mathrm{m/rad}$. When $\omega \geq \omega_0$, $S(\omega)$ decreases rapidly. Therefore, the frequency range of integration is set to be $\omega \in (-10, 10)$rad/m。

In this example, the ETDM and the conventional Monte Carlo simulation (MCS) based on the whole process iteration method (Zhang and Xia 2013) are used for the random vibration analysis of the vehicle-bridge coupled system subjected to random irregularities. The time step used for the ETDM and the MCS is set to be $\Delta t = 0.02s$. The number of samples used in the MCS is $N = 1000$.

To investigate the difference of the dynamic responses between the conventional vehicle model and the simplified vehicle model, the dynamic response under a sample of the random irregularity excitation, which is shown in Fig. 7, is calculated using the whole process iteration method based on the Newmark-β integration scheme (Zhang and Xia 2013). The time history of the vertical displacement in the middle of the bridge is given in Fig. 8. And the time histories of the vertical displacement and the vertical acceleration for the vehicle body are shown in Figs. 9 and 10. As can be seen from Figs. 8-10, it does make no difference in the results of the responses obtained in these figures whether the conventional vehicle model or the simplified vehicle model is used. In addition, the time histories of the angular displacement and the angular acceleration for the vehicle body are given in Figs. 11 and 12. It is noted that the results of conventional vehicle model Figs.

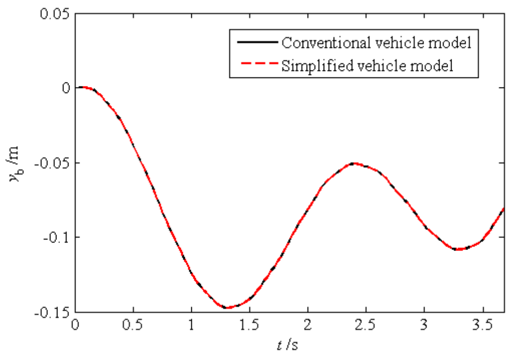

Fig. 8 The time history for the vertical displacement of the bridge span center

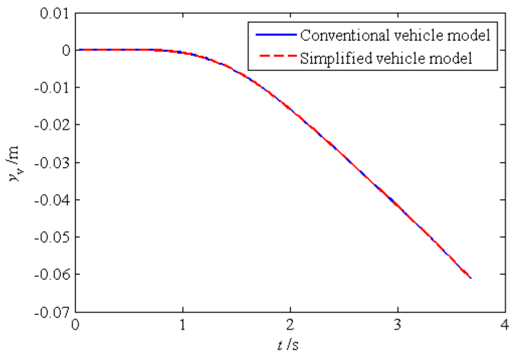

Fig. 9 The time history for the vertical displacement of the vehicle body

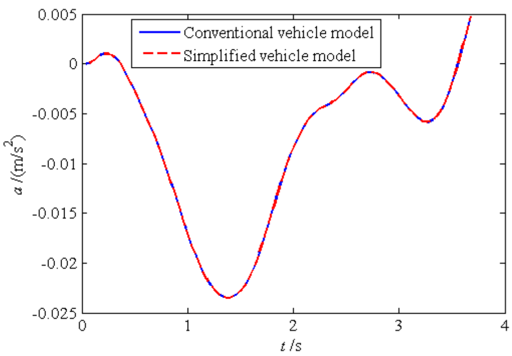

Fig. 10 The time history for the vertical acceleration of the vehicle body

11 and 12 are magnified by 100 times. Precisely because of the existence of the rotational stiffness and the rotational damping for the conventional vehicle model, the angular displacement and the angular acceleration of the vehicle body are constrained. Therefore, the dynamic response of the angular displacement and the angular acceleration is much smaller than that obtained base on the simplified vehicle model. As can be seen from the above analysis, the responses of the vehicle-bridge coupled system can be evaluated well based on the simplified vehicle model without special attention to the degree of freedom for the nodding motion of the vehicle body.

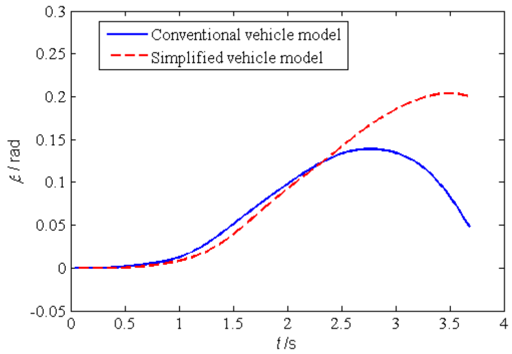

Fig. 11 The time history for the angular displacement of the vehicle body

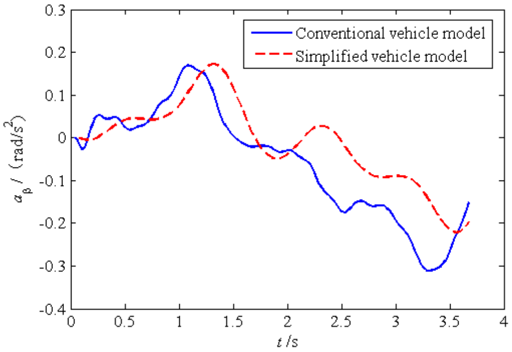

Fig. 12 The time history for the angular acceleration of the vehicle body

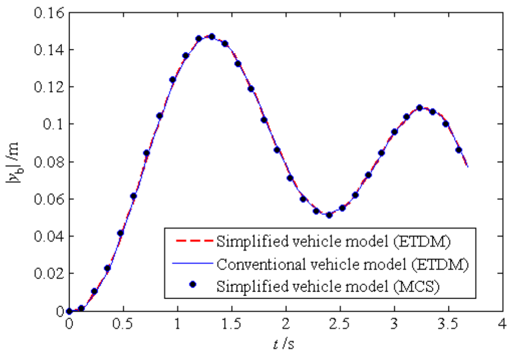

Fig. 13 The absolute mean value time history for the vertical displacement at the bridge span center

Given the validity of the simplified vehicle model, the random dynamic responses of the vehicle-bridge coupled system subjected to random irregularity are calculated based on the ETDM and the MCS, respectively. The time histories of the means and the standard deviations for the mid-span displacement of the bridge subsystem are shown in Figs. 13 and 14, respectively. The time histories of the means and the standard deviations for the vertical displacement and the vertical acceleration of the vehicle body are shown in Figs. 15-18, respectively. As can be seen from Figs. 13-18, the results of the conventional vehicle model and the simplified vehicle model

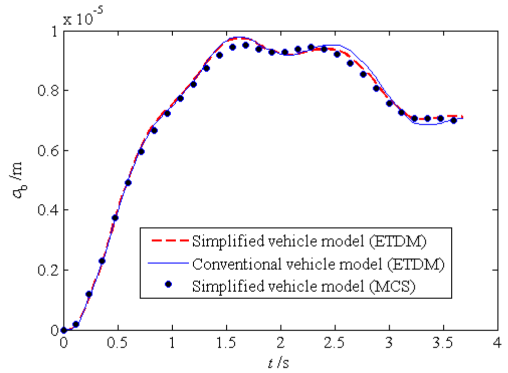

Fig. 14 The standard deviation time history for the vertical displacement at the bridge span center

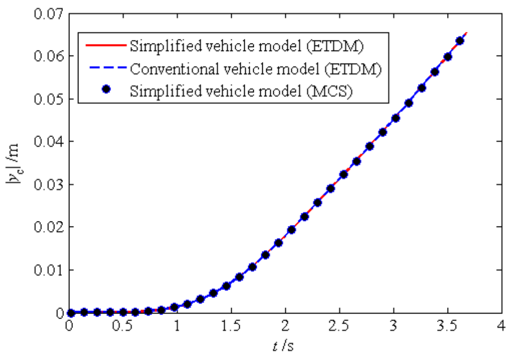

Fig. 15 The absolute mean value time history for the vertical displacement of the vehicle body

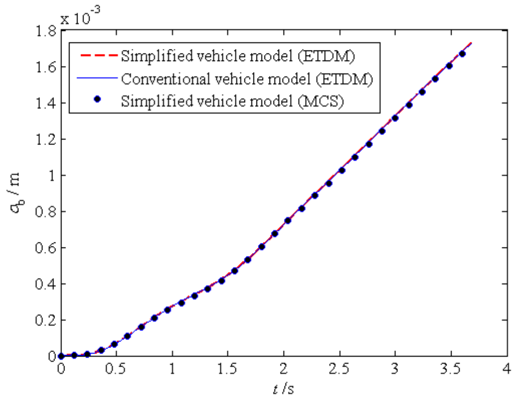

Fig. 16 The standard deviation time history for the vertical displacement of the vehicle body

based on the ETDM are in good agreement compared with that of the simplified vehicle model based on the MCS. The computational efficiency of the ETDM has been already discussed in the literature, e.g., Su *et al.* (2016, 2020), Su and Xu (2014). In this numerical example, the time elapsed by the ETDM is only 20s, while it takes 1720s for the MCS which costs much more time than the ETDM. It is worth noting that the conventional vehicle model and the simplified vehicle

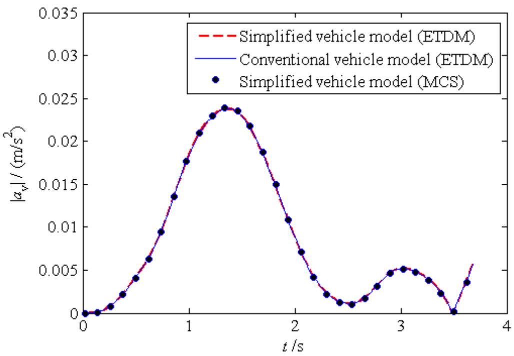

Fig. 17 The absolute mean value time history for the vertical acceleration of the vehicle body

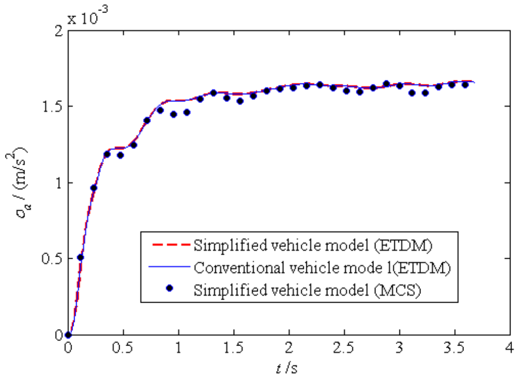

Fig. 18 The standard deviation time history for the vertical acceleration of the vehicle body

model have little influence on the computational efficiency of both the ETDM and the MCS, which can be neglected.

7. Conclusions

For the multi-body model of the vehicle subsystem, the rotational stiffness of the vehicle body and the front-rear bogies are always coupled with their corresponding vertical suspension springs. In this study, a streamlined vehicle model is proposed to eliminate the coupling issue. Numerical results indicate that: (1) when the nodding motion of the vehicle body is overlooked, the results of the other responses of the entire system for the determinate dynamic problem and the random dynamic problem can be evaluated accurately using the simplified vehicle model. In other words, the number of degrees of freedom for the discussed multi-body model can be reduced from 10 to 7 by eliminating the rotational degrees of freedom; (2) The high computational efficiency of ETDM contributes to the benefit of the dimension-reduction analysis for the responses in question.

In future work, the hysteretic nonlinear suspension spring will be incorporated into the simplified vehicle model, and the ETDM-based random vibration analysis of the coupled vehicle-bridge system with local nonlinearities will be conducted. The subsequent studies are consequentially significant for investigating the ride comfort of vehicles with nonlinear suspension and its effect on bridge vibration responses.

Acknowledgment

The research described in this paper was financially supported by Guangdong Basic and Applied Basic Research Foundation, China (Grant No. 2020A1515010611, Grant No. 2021A1515012280).

References

Au, F.T.K., Wang, J.J. and Cheung, Y.K. (2002), "Impact study of cable-stayed railway bridges with random rail irregularities", *Eng. Struct.*, **24**(5), 529-541. https://doi.org/10.1016/S0141-0296(01)00119-5.

Bathe, K.J. (1996), *Finite Element Procedures*, Englewood Cliffs, Prentice-Hall, NJ, USA.

Deng, L., Duan, L.L., He, W. and Ji, W. (2018), "Study on vehicle model for vehicle-bridge coupling vibration of highway bridges in China", *China J. Highw. Transp.*, **31**(7), 92-100. (in Chinese) https://doi.org/10.1590/1679-78251099.

Huang, H., Zheng, H.B., Deng, J.L., Li, W.X. and Li, Y.Y. (2022), "Random analysis of coupled vehicle-bridge systems with local nonlinearities based on explicit time-domain method", *Nonlin. Dyn.*, **108**, 81-95. https://doi.org/10.1007/s11071-021-07190-9.

Lee, H.P. (1994), "Dynamic response of a beam with intermediate point constraints subjected to a moving load", *J. Sound Vib.*, **171**(3), 361-368. https://doi.org/10.1006/jsvi.1994.1126.

Li, J.Q., Leng, X.L. and Fang, T. (2002), "Evolutionary random response problem of a coupled vehicle-bridge system", *Arch. Appl. Mech.*, **72**(6-7), 536-544. https://doi.org/10.1007/s00419-002-0229-6.

Li, W.X. and Ma, H.T. (2019), "A novel model order reduction scheme for fast and accurate material nonlinear analyses of large-scale engineering structures", *Eng. Struct.*, **193**, 238-257. https://doi.org/10.1016/j.engstruct.2019.04.036.

Lu, F., Lin J.H, Kennedy, D. and Williams, F.W. (2009), "An algorithm to study non-stationary random vibration of vehicle-bridge systems", *Compos. Struct.*, **87**, 177-185. https://doi.org/10.1016/j.compstruc.2008.10.004.

Mahmoud, M.A. and Zai, M.A.A. (2002), "Dynamic response of a beam with a crack subject to a moving mass", *J. Sound Vib.*, **256**(4), 591-603. https://doi.org/10.1006/jsvi.2001.4213.

Michaltsos, G., Sophianopoulos, D. and Kounadis, A.N. (1996), "The effect of a moving mass and other parameters on the dynamic response of a simply supported beam", *J. Sound Vib.*, **191**(3), 357-362. https://doi.org/10.1006/jsvi.1996.0127.

Mu, D., Gwon, S.G. and Choi, D.H. (2016), "Dynamic responses of a cable-stayed bridge under a high speed train with random track irregularities and a vertical seismic load", *Int. J. Steel Struct.*, **16**(4), 1339-1354. https://doi.org/10.1007/s13296-016-0104-x.

Pesterev, A.V. and Bergman, L.A. (2000), "An improved series expansion of the solution to the moving oscillator problem", *J. Vib. Acoust.*, **122**(1), 54-61. https://doi.org/10.1115/1.568436.

Podworna, M. and Klasztorny, M. (2014), "Vertical vibrations of composite bridges/track structure/high-speed train systems, Part 2: Physical and mathematical modelling", *Bull. Polish Acad. Sci. Tech. Sci.*, **62**(1), 181-196. https://doi.org/10.2478/bpasts-2014-0019.

Stojanovi, V., Petkovi, M.D. and Deng, J. (2018), "Instability of vehicle systems moving along an infinite beam on a viscoelastic foundation", *Eur. J. Mech. A/Solid.*, **69**(1), 238-254. https://doi.org/10.1016/j.euromechsol.2017.12.007.

Su, C. and Xu, R. (2014), "Random vibration analysis of structures by a time-domain explicit formulation method", *Struct. Eng. Mech.*, **52**(2), 239-260. https://doi.org/10.12989/sem.2014.52.2.239.

Su, C., Huang, H. and Ma, H.T. (2016), "Fast equivalent linearization method for nonlinear structures under nonstationary random excitations", *J. Eng. Mech.*, **142**(8), 04016049. https://doi.org/10.1061/(ASCE)EM.1943-7889.0001094.

Su, C., Huang, H., Ma, H.T. and Xu, R. (2014), "Explicit MCS for random vibration of hysteretic systems by an explicit iteration approach", *Earthq. Struct.*, **7**(2), 119-139. https://doi.org/10.12989/eas.2014.7.2.119

Su, C., Wu, Z.Z. and Xian, J.H. (2020), "Stochastic dynamic analysis of vehicle-bridge coupled systems with nonlinear Hertz contacts by explicit time-domain method", *Vehic. Dyn. Syst.*, **7**, 1-24. https://doi.org/10.1080/00423114.2020.1864418.

Thambiratnam, D. and Zhuge, Y. (1996), "Dynamic analysis of beams on an elastic foundation subjected to moving loads", *J. Sound Vib.*, **198**(2), 149-169. https://doi.org/10.1006/jsvi.1996.0562.

Xiao, X., Yan, Y. and Chen, B. (2019), "Stochastic dynamic analysis for vehicle-track-bridge system based on probability density evolution method", *Eng. Struct.*, **188**, 745-761. https://doi.org/10.1016/j.engstruct.2019.02.042.

Yang, Y.B. and Lin, C.W. (2005), "Vehicle-bridge interaction dynamics and potential applications", *J. Sound Vib.*, **284**(1-2), 205-226. https://doi.org/10.1016/j.jsv.2004.06.032.

Yin, X., Zhi, F., Cai, C.S. and Deng, L. (2010), "Non-stationary random vibration of bridges under vehicles with variable speed", *Eng. Struct.*, **32**(8), 2166-2174. https://doi.org/10.1016/j.engstruct.2010.03.019.

Yu, H.L., Wang, B., Xia, C.P. and Li, Y.L. (2021), "Efficient non-stationary random vibration analysis of vehicle-bridge system based on an improved explicit time-domain method", *Eng. Struct.*, **231**, 111785. https://doi.org/10.1016/j.engstruct.2020.111786.

Yu, Z.W., Mao, J.F., Guo, F.Q. and Guo, W. (2015), "Non-stationary random vibration analysis of a 3D train-bridge system using the probability density evolution method", *J. Sound Vib.*, **366**, 173-189. https://doi.org/10.1016/j.jsv.2015.12.002.

Zhai, W.M. (2015), *Vechicle-Track Coupled Dynamic*, China Science Publishing & Media Ltd, Beijing. (in Chinese)

Zhang, N. and Xia, H. (2013), "A vehicle-bridge interaction dynamic system analysis method based on inter-system iteration", *China Railw. Sci.*, **34**(5), 32-38. (in Chinese) https://doi.org/10.3969/j.issn.1001-4632.2013.05.06.

CC

Nomenclature

v	Travel Speed of the vehicle subsystem
M_c, J_c	Mass and the moment of inertia for the vehicle body
M_t, J_t	Mass and moment of inertia for the front-rear bogies
M_w	Mass of each wheelset
K_{sz}, C_{sz}	Vertical stiffness and damping of the secondary suspension
K_{pz}, C_{pz}	Vertical stiffness and damping of the first suspension
Z_c, Z_{t1}, Z_{t2}, β_c, β_{t1}, β_{t2}	Vertical displacements and the rotational displacements
Z_{wi} ($i = 1, 2, 3, 4$)	Displacement of each wheelset
k_i ($i = 1, 2, 3, 4$)	Stiffness of each wheelset
r_i ($i = 1, 2, 3, 4$)	Irregularity of the bridge deck
$\boldsymbol{M}_v$, $\boldsymbol{K}_v$, $\boldsymbol{C}_v$	Mass matrix, stiffness matrix and damping matrix of the vehicle subsystem
$\boldsymbol{Y}_v$, $\dot{\boldsymbol{Y}}_v$, $\ddot{\boldsymbol{Y}}_v$	Displacement, velocity and acceleration vector of the vehicle

	subsystem
$\boldsymbol{L}_v$, $\boldsymbol{L}_b(x)$	Position matrix
$\boldsymbol{F}(t)$	Vehicle-bridge contact force function
$\boldsymbol{F}_{1-j}$	Contact force vector from t_1 to t_j
$\boldsymbol{M}_b$, $\boldsymbol{C}_b$, $\boldsymbol{K}_b$	Mass matrix, damping matrix and stiffness matrix of the bridge subsystem
$\boldsymbol{Y}_b$, $\dot{\boldsymbol{Y}}_b$, $\ddot{\boldsymbol{Y}}_b$	Displacement vector, velocity vector and acceleration vector of the bridge subsystem
g	Gravity acceleration
$\boldsymbol{G}$	Gravity vector
G	Gravity value
$y_{\mathrm{v},\,i}(t)$ $(i = 1, 2, 3, 4)$	Vertical displacement of the i-th wheelset
$y_{\mathrm{b},\,i}(x, t)$ $(i = 1, 2, 3, 4)$	Vertical displacement of the bridge deck
$r_i(x)$ $(i = 1, 2, 3, 4)$	Irregularity of the bridge deck corresponding to the i-th wheelset
γ, β	Two parameters used to control the Newmark-β integration stability
$\boldsymbol{A}_{\mathrm{v}(j,p)}$ $(p = 1,2,\cdots,j)$	Coefficient matrices of responses for the vehicle subsystem
$\boldsymbol{A}_{b(j,p)}$	Coefficient matrices of responses for the bridge subsystem
$\boldsymbol{V}_v(t_j)$	State vector of vehicle subsystem
$\boldsymbol{V}_b(t_j)$	State vector of the bridge subsystem
$\boldsymbol{y}_{\mathrm{v},\,1\text{-}n}$	The displacements of the four wheelsets from t_1 to t_n
$\boldsymbol{y}_{\mathrm{b},\,1\text{-}n}$	Vertical displacements of the bridge deck corresponding to the wheel-bridge contact points
$\tilde{y}_v$	Response of the vehicle subsystem
$\tilde{y}_b$	Response of the bridge subsystem